



Novel synthesis of manganese and vanadium mixed oxide (V₂O₅/OMS-2) as an efficient and selective catalyst for the oxidation of alcohols in liquid phase



Vahid Mahdavi*, Shima Soleimani

Department of Chemistry, Surface Chemistry and Catalysis Division, Faculty of Sciences, Arak University, Arak 38156-8-8349, Iran

ARTICLE INFO

Article history:

Received 27 February 2013
Received in revised form 12 November 2013
Accepted 15 November 2013
Available online 23 November 2013

Keywords:

D. Catalytic properties
A. Microporous materials
A. Oxides
A. Composites, C. X-ray diffraction

ABSTRACT

This work reports the synthesis and characterization of mixed oxide vanadium–manganese V₂O₅/K-OMS-2 at various V/Mn molar ratios and prepared by the impregnation method. Characterization of these new composite materials was made by elemental analysis, BET, XRD, FT-IR, SEM and TEM techniques. Results of these analyses showed that vanadium impregnated samples contained mixed phases of cryptomelane and crystalline V₂O₅ species.

Oxidation of various alcohols was studied in the liquid phase over the V₂O₅/K-OMS-2 catalyst using *tert*-butyl hydroperoxide (TBHP) and H₂O₂ as the oxidant. Activity of the V₂O₅/K-OMS-2 samples was increased considerably with respect to K-OMS-2 catalyst due to the interaction of manganese oxide and V₂O₅.

The kinetic of benzyl alcohol oxidation using excess TBHP over V₂O₅/K-OMS-2 catalyst was investigated at different temperatures and a pseudo-first order reaction was determined with respect to benzyl alcohol. The effects of reaction time, oxidant/alcohol molar ratio, reaction temperature, solvents, catalyst recycling potential and leaching were investigated.

© 2013 Elsevier Ltd. All rights reserved.

1. Introduction

The transformation of alcohols into aldehydes or ketones is a fundamental reaction in organic synthesis [1]. A number of methods are commonly applied for alcohol oxidation, however the development of newer methods and methodologies is currently gaining much attention due to the importance such reactions.

Recently there has been increased research attention directed at developing heterogeneous catalysts for the oxidation of alcohols in the liquid phase with molecular oxygen, aqueous hydrogen peroxide or organic peroxides. These oxidants are very efficient and environmentally friendly as the only by-products are water or alkyl alcohols. The pathway of heterogeneous catalytic oxidation is more acceptable than that of homogeneous reactions because the solid catalysts in heterogeneous oxidation reactions are easily recovered, or can be used in a continuous process.

Vanadium containing molecular sieves was found to be an active ingredient in a number of liquid phase oxidation reactions in the presence of dilute hydrogen peroxide or *tert*-butyl

hydroperoxide (TBHP), such as, the hydroxylation of aromatic compounds [2], the oxidation of alkanes [3,4], the sulfoxidation of thioethers [5] and the oxidation of amines [6].

However, manganese oxide octahedral molecular sieves (OMS-2) are a nonporous tunnel-structured material. Research has determined that these mixed valent materials are effective catalysts in oxidation reactions [7–11].

The K⁺ ion form of OMS-2 (hollandite) which is known as cryptomelane, has a composition of KMn₈O₁₆·nH₂O [12]. Synthetic cryptomelane (OMS-2) has the structural unit MnO₆ octahedra, edge and corner shared, similar to the hollandite structure with K⁺ as the predominant cation in the tunnel (Fig. 1). The structure contains 4.6 Å × 4.6 Å tunnels because of the 2 × 2 arrangement of octahedra and K⁺ ion with a small amount of water present in the tunnel. The average manganese oxidation state OMS-2 is 3.8 due to the presence of a mixture of Mn⁴⁺, Mn³⁺, and Mn²⁺ ions [13–15]. The mixed valence of OMS-2 along with the one-dimensional tunnel structure is capable of exhibiting interesting oxidation properties [7–11]. In comparison to other manganese coordination complexes [16–18], manganese oxides with a cryptomelane structure are appropriate because preparation is simple and inexpensive. These materials have already shown good catalytic activity in the case of alcohol oxidation reaction [11,19]. Divalent and trivalent transition metal ion incorporated cryptomelane

* Corresponding author. Fax: +98 863 4173406.

E-mail addresses: v-mahdavi@araku.ac.ir, vmahdavius@yahoo.com (V. Mahdavi).

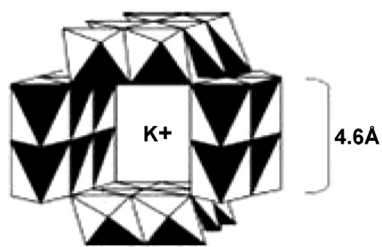


Fig. 1. Structure of K-OMS-2, which is synthetic cryptomelane $\text{KMn}_8\text{O}_{16}\cdot n\text{H}_2\text{O}$.

M-OMS-2 is an example of a recently developed catalyst that improved oxidation for alcohols and side chains in organic compounds [20].

This work is the first report on the synthesis of some vanadium oxide containing nano porous manganese oxide octahedral molecular sieves ($\text{V}_2\text{O}_5/\text{K-OMS-2}$) with different V/Mn molar ratios and the oxidation of alcohols investigated in the liquid phase over $\text{V}_2\text{O}_5/\text{K-OMS-2}$ samples using *tert*-butyl hydro peroxide (TBHP) or hydrogen peroxide as the oxidant. The report proposes that there is a relationship between structure and catalytic performance and on the effect of the V/Mn molar ratio. For the kinetic study of oxidation, benzyl alcohol was chosen as a substrate for the model and the effects of reaction time, oxidant/alcohol molar ratio, temperature, solvents, catalyst recycling and leaching were investigated.

2. Experimental

2.1. Materials

All reagents used in the experiment were of the highest commercial quality, and purchased from Aldrich and Merck chemical companies and used without further purification.

2.2. Preparation of catalysts

Cryptomelane type of parent tunneled structure manganese oxide OMS-2 was prepared by the precipitation method [7,21]. A 0.4 M solution of KMnO_4 (13.3 g in 225 mL of distilled water, DDW) was added to a mixture of a 1.75 M solution of $\text{MnSO}_4\cdot\text{H}_2\text{O}$ (19.8 g in 67.5 mL DDW) and 6.8 mL of concentrated HNO_3 . The resulting black precipitate was stirred vigorously and refluxed at 373 K for 24 h. The precipitate was filtered and washed with DDW until neutral pH was reached and it was then dried at 393 K. This gave the K^+ form of OMS-2, which was shown to be K-OMS-2.

Samples of vanadium containing K-OMS-2 catalysts were prepared by impregnation described as follows; 1 g of K-OMS-2 was dispersed in water (50 mL) containing the required amount of NH_4VO_3 (x g) and oxalic acid (1 g). The mixture was stirred and evaporated at 65 °C until dry and calcined at 673 K for 4 h under airflow. Evaluations for contents of manganese and vanadium were determined by atomic absorption spectroscopy (AAS) using a Perkin-Elmer Analyst instrument, after extraction of metals from the sample catalysts in HNO_3 and HF acids.

The V/Mn molar ratio ranged from 1.15 to 3.64 (Table 2) and $\text{V}_2\text{O}_5/\text{K-OMS-2}(1.15)$ stands for the vanadium containing K-OMS-2 catalyst with V/Mn = 1.15.

In the next step these solids ($\text{V}_2\text{O}_5/\text{K-OMS-2}$) were used in liquid phase to catalyze the oxidation of alcohols by TBHP.

2.3. Characterization of catalyst

Surface area and pore size distribution of K-OMS-2 and $\text{V}_2\text{O}_5/\text{K-OMS-2}$ catalysts were determined by N_2 adsorption-desorption

measurement at 77 K using a Micromeritics ASAP 2010 instrument. Before starting the process of nitrogen adsorption, each sample was outgassed at 250 °C under vacuum for 8 h. Evaluation of surface area was made according to data on nitrogen adsorption determined by the Brunauer-Emmett-Teller (BET) method and pore size distribution was estimated using the method of Barrett-Joyner-Halenda (BJH). Catalyst structure was determined by X-ray diffraction (XRD) tests. A diffractometer Philips model PW 1800 instrument with $\text{Cu K}\alpha$ radiation and Ni filter was used to collect X-ray data. The SEM images were obtained with a Philips XL30 instrument. Transmission electron microscopy (TEM) images were collected on a JEOL 2010 electron microscope operated at an acceleration voltage of 100 kV. Samples were made by grinding using a pestle and mortar, followed by dispersion in ethanol, sonicated and then dropped into a wholly carbon-coated copper grid. The infrared spectrum was recorded on a Galaxy Ft-IR 500 spectrophotometer.

2.4. Oxidation of alcohols

In a typical procedure, a mixture of 0.2 g catalyst with the grain size of 200–230 mesh, 15 mL solvent (acetonitrile) and 30 mmol of alcohol (benzyl alcohol, cyclohexanol or *n*-hexanol) was stirred in a three-necked flask under nitrogen atmosphere at 50 °C for 30 min. The stirring rate of the solution was set at 750 cycle/min. Then 30 mmol of the oxidant (TBHP) was added. The mixture was refluxed at 90 °C for 8 h under nitrogen atmosphere (Table 2). After filtration, the solid was washed with CH_2Cl_2 and the reaction mixture was analyzed by GC. A GC-MS model Thermo Finnigan (60 m, RTX-1 column) was used for identification of products and a GC (Perkin-Elmer Model 1800) was used for product analysis. The GC was equipped with a flame ionization detector (FID) connected to a 3% OV-17 column with length of 2.5 m and diameter of 1/8 in.

3. Results and discussion

3.1. Characterization of the $\text{V}_2\text{O}_5/\text{K-OMS-2}$ catalysts

Fig. 2(A) and (B) shows the nitrogen adsorption-desorption isotherms of the K-OMS-2 and $\text{V}_2\text{O}_5/\text{K-OMS-2}(2.30)$ samples. These isotherms corresponded to type II on the IUPAC classification system [22]. The isotherm of $\text{V}_2\text{O}_5/\text{K-OMS-2}(2.30)$ sample exhibited hysteresis loops (type H3) with sloping adsorption and desorption branches covering a large range of P/P_0 [22]. Pore size distribution was analyzed using the BJH adsorption method (Fig. 2(C)). The adsorption branch was located at relative pressures in the range of 0.2–1.0. A wide pore diameter distribution with a mean value of 13.8 nm was obtained by the BJH adsorption method.

Since the K-OMS-2 and $\text{V}_2\text{O}_5/\text{K-OMS-2}$ compound contained micropores, nitrogen adsorption isotherm data were also applied to the D-R (Dubinin-Radushkevich) isotherm model to evaluate total micro pores volume W_0 and D (a constant characteristic of the pore size distribution). The linear form of the D-R isotherm equation is:

$$\ln V = \ln \left(\frac{W_0}{1.558 \times 10^{-3}} \right) - D \left[\ln \frac{P}{P_0} \right]^2$$

where D is $A(RT/\beta)^2$, A is a constant and β is known as an affinity coefficient. A plot of $\ln V$ vs. $[\ln(P/P_0)]^2$ gives a straight line of slope D and intercept $\ln(W_0/1.558 \times 10^{-3})$ over the relative pressure range $1 \times 10^{-5} < P/P_0 < 0.2$.

Evaluations of surface area, pore volume, W_0 and D of OMS-2 and $\text{V}_2\text{O}_5/\text{K-OMS-2}(2.3)$ samples are shown in Table 1.

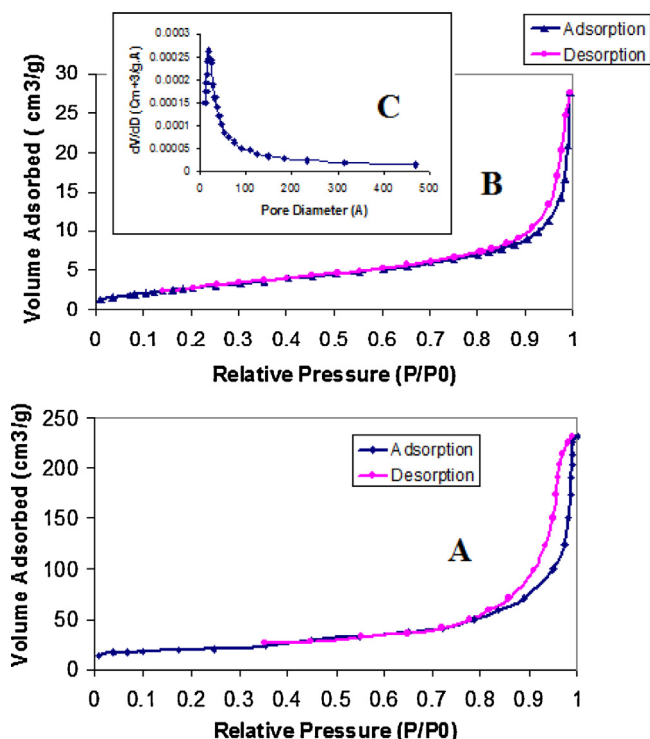


Fig. 2. N₂ adsorption/desorption isotherms at 77 K for (A) K-OMS-2, (B) V₂O₅/K-OMS-2(2.30), (C) BJH analysis of the distribution of pore size in V₂O₅/K-OMS-2(2.30).

XRD patterns of the OMS-2 and vanadium impregnated catalyst after calcinations, V₂O₅/K-OMS-2 with different V/Mn molar ratios are shown in Fig. 3. The intense reflections of the patterns reveal a high level of crystallinity. The XRD pattern (Fig. 3(A)) and the major *d* spacing values of synthesized OMS-2 sample were matched with the reported data of OMS-2 type manganese oxide crystal structure such as cryptomelane. The XRD spectra of this sample agree with those reported in the related literature [23].

XRD patterns of the V₂O₅/K-OMS-2 with different V/Mn molar ratios are shown in Fig. 3(B)–(E), and correspond to a mixture of V₂O₅ and K-OMS-2. The XRD spectra in Fig. 3(C) shows high intensity peaks at 2θ values of 15.10°, 20.23°, 22.03°, 26.12°, 31.10°, 33.15°, 34.13°, 47.16°, 51.95°, 61.56° and 62.16°, characteristic of the presence of a V₂O₅ phase. XRD spectra also show high intensity peaks at 2θ values of 11.12°, 13.03°, 18.30°, 28.60°, 37.96°, 42.40°, 50.11°, 56.15° and 60.17° which are characteristic of the presence of a cryptomelane phase. The diffraction pattern of this sample indicates the presence of mixed phases of cryptomelane and V₂O₅ without any other phase. However, intensity of the OMS-2 XRD pattern decreased according to an increased V/Mn molar ratio (Fig. 3(B)–(E)) and Fig. 3(D) and (E) indicates that OMS-2 is amorphous or remains in a highly dispersed state on the V₂O₅/OMS-2 system.

SEM micrographs of K-OMS-2 and V₂O₅/K-OMS-2 samples with different V/Mn molar ratios are given in Fig. 4. Fig. 4(A) shows OMS-2 with a fibrous; needle-like morphology and this is in

Table 1

Surface area, pore volume and D–R isotherm parameters of OMS-2 and V₂O₅/K-OMS-2(2.3) samples.

Sample	S _{BET} (m ² /g)	Pore volume (cm ³ /g)	W ₀ (cm ³ /g)	D
K-OMS-2	85	0.361	0.0292	0.0125
V ₂ O ₅ /K-OMS-2(2.3)	10.45	0.042	0.0046	0.0734

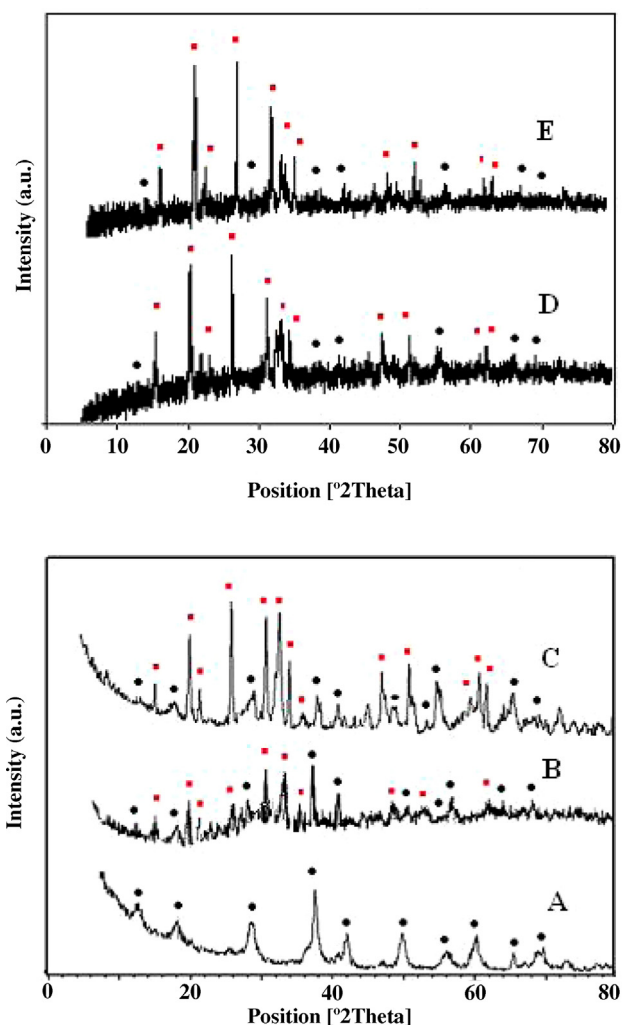


Fig. 3. X-ray diffraction patterns of (A) K-OMS-2, (B) V₂O₅/K-OMS-2(1.15), (C) V₂O₅/K-OMS-2(2.30), (D) V₂O₅/K-OMS-2(2.80) and (E) V₂O₅/K-OMS-2(3.64). Peaks due to (■) V₂O₅ phase and (●) cryptomelane KMn₈O₁₆·nH₂O phase.

agreement with the results obtained in the work of Makwana et al. [24]. However, SEM micrographs of V₂O₅/K-OMS-2 samples (Fig. 4(B)–(F)) clearly show mixtures of V₂O₅ particles with rod-like morphology and OMS-2 aggregated particles, which are in agreement with the results observed in XRD tests. As seen in Fig. 4(B)–(E), the addition of vanadium to OMS-2, changed the main morphology of samples such that particle size of the V₂O₅ crystals decreased according to an increased V/Mn molar ratio.

Results of transmission electron microscopy (TEM) tests for K-OMS-2 and V₂O₅/K-OMS-2(2.30) are shown in Fig. 5(A) and (B), respectively. Fig. 5(B) shows the presence of mixed phases of the tunnel structure of OMS-2 and V₂O₅ particles with rod-like morphology. As seen in Fig. 5(A) and (B), size of the OMS-2 crystals decreased under pure K-OMS-2. Results of the TEM tests on these samples show that rod-like length mostly ranged from 20 to 200 nm in size.

Fig. 6 shows the FT-IR spectra of the K-OMS-2 and V₂O₅/K-OMS-2 samples.

The FT-IR spectra of cryptomelane OMS-2 contains some characteristic bands associated with Mn–O peaks, at about 468, 522.7 and 711.78 cm⁻¹.

Fig. 6 demonstrates that there was no significant difference in terms of FT-IR spectra obtained from the V₂O₅/K-OMS-2 samples and characteristic vanadium peaks were evident at 295, 356, 1020 and 1291 cm⁻¹.

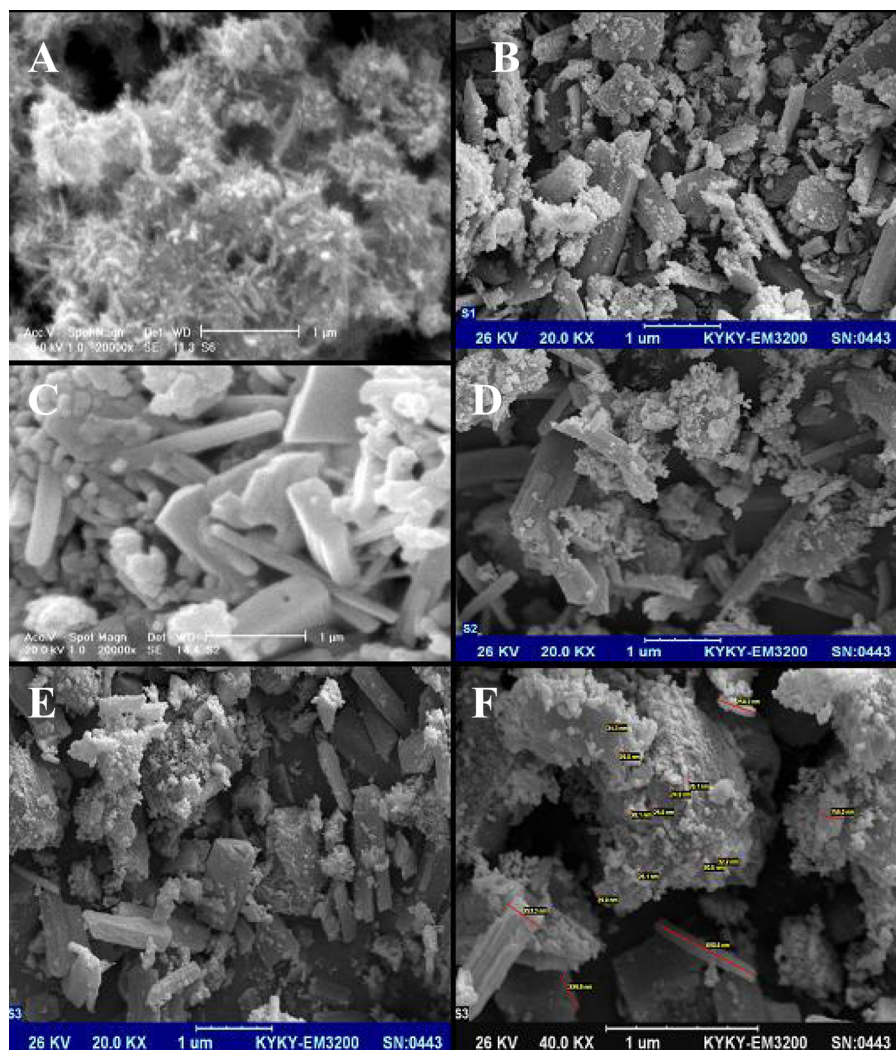


Fig. 4. Scanning electron micrograph of (A) K-OMS-2, (B) $V_2O_5/K-OMS-2(1.15)$, (C) $V_2O_5/K-OMS-2(2.30)$, (D) $V_2O_5/K-OMS-2(2.80)$, (E) $V_2O_5/K-OMS-2(3.4)$ and (F) $V_2O_5/K-OMS-2(3.4)$ with higher magnification.

3.2. Oxidation of benzyl alcohol with TBHP

Firstly, the model compound benzyl alcohol was tested for reactivity under a variety of experimental conditions. Results for oxidation of benzyl alcohol with TBHP in the presence of K-OMS-2, $V_2O_5/K-OMS-2$ with 1.15, 2.30, 2.80, and 3.64 of V/Mn molar ratio, are shown in Table 2. All reactions were conducted at reflux temperature ($90^\circ C$) for 8 h with 0.2 g of catalyst, 15 mL of solvent, 30 mmol of benzyl alcohol and 30 mmol TBHP. The conversion percentage was calculated for all reactions according to amounts of substrate (benzyl alcohol). The results show that reactions with $V_2O_5/K-OMS-2$ catalysts had relatively high conversion percentages compared to K-OMS-2 sample. In addition, reactions that involved the $V_2O_5/K-OMS-2(2.30)$ catalyst had higher activity with respect to other samples with 1.15, 2.80, and 3.64 of V/Mn molar ratio. Table 2 shows that selectivity of all catalysts was independent of the system of catalysis and an increasing loading of vanadium on the K-OMS-2 catalyst, and that selectivity with respect to benzaldehyde remained constant.

On the $V_2O_5/K-OMS-2(2.30)$ catalyst, the conversion of benzyl alcohol was 79.94% and selectivity of benzaldehyde was 100%. Therefore $V_2O_5/K-OMS-2(2.30)$ can be determined as a better catalyst compared with the other catalysts listed in Table 2.

In fact, the results of these catalytic tests showed that the vanadium impregnated catalyst had greatly enhanced catalytic

activity compared to the K-OMS-2 sample due to the interaction of manganese oxide and V_2O_5 and that was possibly due to a synergistic effect. The oxidation of benzyl alcohol with TBHP and O_2 over the various catalytic systems is given in Table 3. In comparison with catalysts reported in previous work [25,26], the $V_2O_5/K-OMS-2(2.30)$ sample tested in this study had as higher level of activity than catalysts reported in our previous studies, and it had comparable catalytic activity to catalytic systems reported on other research [27–35]. For our catalytic system, the selectivity with respect to aldehydes was 100%. Therefore, tests determined that this catalytic system is suitable for application in the oxidation reaction of alcohols.

3.3. Effect of oxidant/alcohol molar ratio

This experiment evaluated change in the conversion (%) of benzyl alcohol in the presence of TBHP oxidant and $V_2O_5/K-OMS-2(2.30)$ catalyst with 1, 2 and 3 TBHP/benzyl alcohol molar ratios (Table 4). The reaction was carried out at reflux temperature ($90^\circ C$) using 0.2 g of catalyst, 15 mL of acetonitrile and three different amounts of TBHP viz. 30, 60 and 90 mmol for a fixed amount of benzyl alcohol (30 mmol) and reaction time (8 h).

The conversion percentage increased according to an increment of TBHP to benzyl alcohol molar ratio. However, selectivity of benzaldehyde decreased due to the consecutive reaction of the

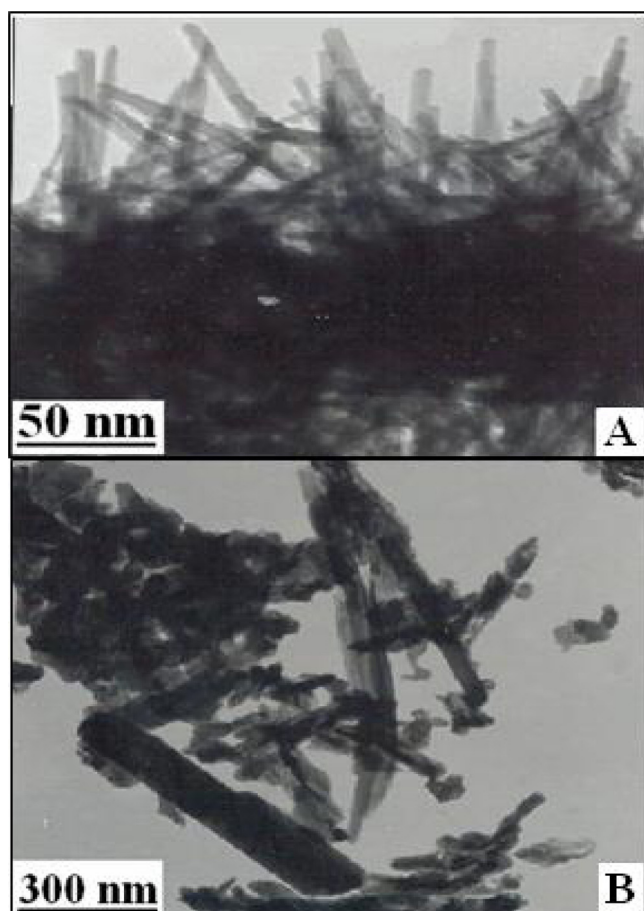


Fig. 5. TEM picture of (A) K-OMS-2 and (B) $V_2O_5/K-OMS-2(2.30)$.

transformation of benzaldehyde to benzoic acid. The lowest TBHP/benzyl alcohol ratio, resulted in 79.94% conversion of benzyl alcohol and 100% selectivity to benzaldehyde and the highest TBHP/benzyl alcohol ratio (3:1), produced 93.53% conversion and 41.10% and 58.90% selectivity to benzaldehyde and benzoic acid, respectively.

Table 4 shows that the conversion of benzyl alcohol increased up to 92% without any inhibitory effect.

3.4. Effect of substrates and oxidants on oxidation

In this study, tests were done on various selected alcohols. Conversion percentage and selectivity of the products are compared in Table 5. The highest conversion (%) was obtained

Table 2

Oxidation of benzyl alcohol with TBHP in the presence of $V_2O_5/K-OMS-2$ catalyst. Reaction condition: 0.2 g catalyst with the grain size of 200–230 mesh; stirring rate of the reaction mixture 750 cycle/min; benzyl alcohol 30 mmol; TBHP 30 mmol; 15 mL acetonitrile; reflux temperature (90 °C); reaction time 8 h.

Catalyst	V/Mn ^a (molar ratio)	Selectivity of benzaldehyde (%)	Conversion (%) of benzyl alcohol
K-OMS-2	0	100	50.82 (0.58) ^b
$V_2O_5/K-OMS-2(1.15)$	1.15	100	62.75 (1.30)
$V_2O_5/K-OMS-2(2.30)$	2.30	100	79.94 (0.73)
$V_2O_5/K-OMS-2(2.80)$	2.80	100	60.85 (0.78)
$V_2O_5/K-OMS-2(3.64)$	3.64	100	62.50 (1.07)

Selec._i=(moles of benzyl alcohol converted to *i*/moles of benzyl alcohol reacted) × 100. Conver._i=(moles of benzyl alcohol reacted/moles of benzyl alcohol in the feed) × 100.

^a The contents of Mn and V were determined by AAS.

^b The numbers in parentheses indicate standard deviation (S).

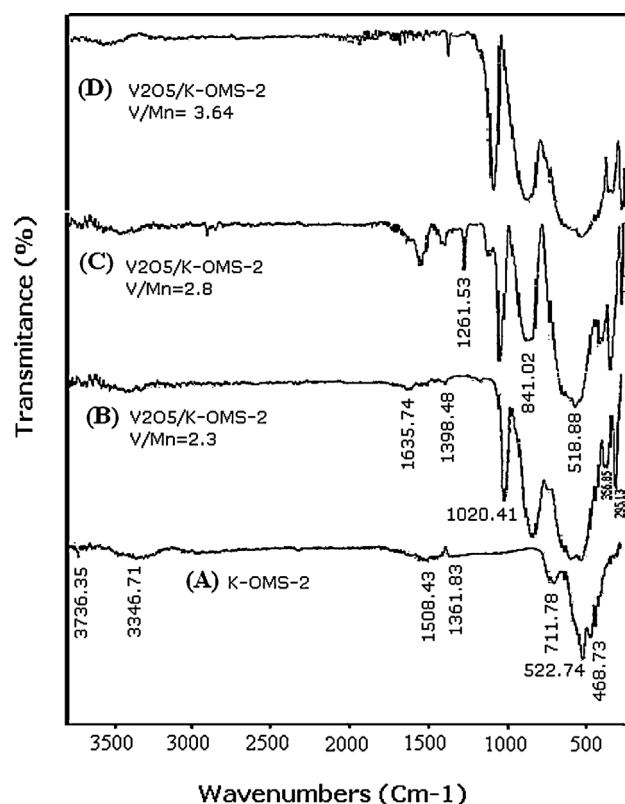


Fig. 6. FT-IR spectra of (A) K-OMS-2, (B) $V_2O_5/K-OMS-2(2.30)$, (C) $V_2O_5/K-OMS-2(2.80)$ and (D) $V_2O_5/K-OMS-2(3.64)$.

for benzyl alcohol on $V_2O_5/K-OMS-2(2.30)$ catalyst using TBHP oxidant. Table 5 shows that reactivity of the alcohols toward oxidation with TBHP and H_2O_2 on the $V_2O_5/K-OMS-2(2.30)$ catalyst depends on the particular structure of the substrate. It shows that TBHP is more efficient oxidant due to having a weaker O–O band with respect to H_2O_2 . The order of reactivity of the alcohols, benzyl alcohol > n-hexanol > cyclohexanol > 2-ethyl-1-hexanol, clearly related to steric hindrance of the alcohol function.

3.5. Effect of solvents

In these experiments the solvent was changed for each run, while the other conditions (0.2 g of the $V_2O_5/K-OMS-2(2.30)$ catalyst, 30 mmol benzyl alcohol, 30 mmol TBHP, stirring rate of the reaction mixture 750 cycle/min and reaction temperature, 70 °C for 8 h) remained the same. The solvent has been varied from a polar to a nonpolar state. Results of conversion of benzyl alcohol with the various solvents are shown in Table 6.

As demonstrated in Table 6, the behavior of benzyl alcohol oxidation in various solvents was strikingly different. The conversion (%) of benzyl alcohol decreased in the order: acetonitrile > toluene > THF > ethanol with 100% selectivity to benzaldehyde.

Acetonitrile is a polar solvent with a very high dielectric constant; it may readily dissolve TBHP along with the benzyl alcohol and increasing the efficiency of the catalytic system. Also, highly polar solvents like acetonitrile may facilitate formation of active oxygen species and thereby enhance the catalytic activity.

3.6. Kinetics of reaction

Oxidation of benzyl alcohol was studied exclusively for kinetic evaluation and results of the study are as follows.

Table 3
Benzyl alcohol oxidation using various heterogeneous catalysts.

Catalyst	Oxidant	Time (h)	Benzyl alcohol conversion (%)	Selectivity of aldehyde (%)	Reference
V ₂ O ₅ /K-OMS-2(2.30)	TBHP	8	79.9	100	Our catalyst
[Mn(bpy) ₂] ²⁺ /HMS	TBHP	8	49.2	100	[25]
[Co(bpy) ₂] ²⁺ /bentonite	TBHP	8	53	100	[26]
CuCl	O ₂	48	1.2	50	[27]
MCM-41-TEMPO/CuCl ^a	O ₂	48	35	99	[27]
H ₅ PV ₂ Mo ₁₀ O ₄₀	O ₂	6	8.4	100	[28]
RuO ₂	O ₂	1.5	16	99	[29]
Mn-Cr-HT ^b	O ₂	–	18.7	99.5	[30]
PdO-CuO·3H ₂ O	O ₂	1	45	98	[31]
CuCl ₂	TBHP	17	20	–	[32]
Fe-Phen-MCM-41 ^c	TBHP	20	34.9	–	[33]
Mn-Cr-LDH ^d	TBHP	5	49.8	83.5	[34]
Co-Cr-LDH	TBHP	5	59.5	70	[34]
Ru1.9/TiO ₂	TBHP	1	30	82	[35]

^a 2,2,6,6-Tetramethylpiperidine-N-oxyl known as TEMPO.

^b HT hydrotalcite like solid catalyst.

^c Phenanthroline known as Phen.

^d Layered double hydroxides known as LDH.

Table 4

Effect of oxidant/substrate ratio. Reaction condition: 0.2 g V₂O₅/K-OMS-2(2.30) catalyst; benzyl alcohol 30 mmol; oxidant (TBHP) 30, 60 and 90 mmol; 15 mL solvent (acetonitrile); stirring rate of the reaction mixture 750 cycle/min; reflux temperature (90 °C); reaction time 8 h.

TBHP/benzyl alcohol molar ratio	Conversion of benzyl alcohol (%)	Selectivity of benzaldehyde (%)
1:1	79.94 (0.73) ^a	100
2:1	85.81 (1.24)	63.20 ^b
3:1	93.53 (0.68)	41.10 ^c

Conver. = (moles of benzyl alcohol reacted/moles of benzyl alcohol in the feed) × 100. Selec._{*i*} = (moles of benzyl alcohol converted to *i*/moles of benzyl alcohol reacted) × 100.

^a The numbers in parentheses indicate standard deviation (*S*).

^b Selectivity of benzoic acid is 36.80%.

^c Selectivity of benzoic acid is 58.90%.

In this kinetic study the depletion of benzyl alcohol concentration in the presence of excess TBHP was monitored and plotted with respect to time (Fig. 7(A)). The reaction was carried out in a mixture of 15 mL acetonitrile, 10 mmol benzyl alcohol, 150 mmol TBHP and 0.2 g of V₂O₅/K-OMS-2(2.30) catalyst with the grain size of 200–230 mesh and stirring rate of the reaction mixture 750 cycle/min at 90 °C in a two-necked round bottom flask. Samples of 0.3 μL were withdrawn at regular intervals and analyzed by GC. The rate expression [36] may be written as:

$$\text{Rate} = k[\text{BZOH}]^n[\text{TBHP}]^m \quad (1)$$

where BZOH stands for benzyl alcohol, *n* is the order of reaction with respect to benzyl alcohol, *m* is the order of reaction with respect to TBHP, and *k* is the rate constant. If *n* = 1 and using excess concentration of TBHP, the integrated expression can be written as

$$-\ln(1 - X) = k't, \quad (2)$$

X is the conversion of benzyl alcohol after time *t*.

Table 5

Effect of the V₂O₅/K-OMS-2(2.30) catalyst in the oxidation of different alcohols. Reaction condition: 0.2 g catalyst; alcohol 30 mmol; oxidant TBHP 30 mmol; 15 mL acetonitrile; stirring rate of the reaction mixture 750 cycle/min; reflux temperature (90 °C); reaction time 8 h.

Alcohol	Product	Conversion (%)		Selectivity (%)
		TBHP oxidant	H ₂ O ₂ oxidant	
Benzyl alcohol	Benzaldehyde	79.94 (0.73) ^a	34.71 (0.93)	100
n-Hexanol	Hexanal	65.75 (0.97)	23.80 (0.71)	100
Cyclohexanol	Cyclohexanone	49.11 (0.79)	26.11 (1.12)	100
2-Ethyl-1-hexanol	2-Ethyl-1-hexanal	43.04 (0.65)	28.83 (0.58)	100

^a The numbers in parentheses indicate standard deviation (*S*).

According to expression (2), the plot of $-\ln(1 - X)$ with respect to time gives a linear relationship and as such represents a pseudo-first-order dependence on benzyl alcohol. The kinetic of benzyl alcohol oxidation at reflux temperature (90 °C) was investigated and according to Fig. 7(B), it followed a pseudo-first order with respect to benzyl alcohol.

3.6.1. Effect of temperature on the rate of the oxidation of benzyl alcohol

Oxidation of benzyl alcohol was carried out at 26, 45, 60, 75 and 90 °C in the same reaction conditions and rate constants of reactions were determined, these are shown in Fig. 7(A) and (B). Evaluations of regression analysis, by fitting function LINEST (Excel Software) for data of Fig. 7(B), are shown in Table 7. These results suggest that oxidation of benzyl alcohol over the V₂O₅/K-OMS-2 catalyst well follows the pseudo-first order kinetic model.

From the pseudo-first-order rate constants, the plot of $\ln k'$ vs. $1/T$ (Arrhenius plot) was drawn (Fig. 8) and the value of the apparent activation energy (*E_a*) was evaluated from the slope of the plot, it was determined as 22.2 kJ mol⁻¹.

3.7. Catalyst recycling and leaching

The catalyst V₂O₅/K-OMS-2(2.30) was selected for tests and benzyl alcohol was used as a model substrate for evaluating recycling and leaching. Leaching of the catalyst was tested by filtering the catalyst during the reaction and checking the conversion progress in the filtrate solution. In this study, a mixture of 0.2 g catalyst V₂O₅/K-OMS-2(2.30), 15 mL acetonitrile, 30 mmol TBHP and 30 mmol of benzyl alcohol, was refluxed for 4 h and conversion of 61.2% was obtained. Then the reaction mixture was filtered and then the filtrate solution was refluxed for the next 4 h and the conversion level of 65.3% was obtained. In comparison, another experiment was carried out by refluxing the initial

Table 6

Effect of solvents on oxidation of benzyl alcohol. Reaction condition: 0.2 g V₂O₅/K-OMS-2(2.30) catalyst; benzyl alcohol 30 mmol; oxidant TBHP 30 mmol; 15 mL solvent; stirring rate of the reaction mixture 750 cycle/min; reaction temperature 70 °C; reaction time 8 h.

Solvent	Dielectric constant	Dipole moment (D)	Conversion (%)	Selectivity (%)
Acetonitrile	37.5	3.92	79.94 (0.73) ^a	100
THF	7.5	3.89	58.62 (0.54)	100
Ethanol	24.5	1.69	46.35 (0.82)	100
Toluene	2.4	0.37	62.12 (0.32)	100

^a The numbers in parentheses indicate standard deviation (S).

Table 7

The regression analysis by fitting function LINEST (Excel Software).

T (°C)	Equation of line	k' (min ⁻¹)	Standard error of k'	R ²	SS _{resid}
26	Y=0.0900X	0.0900	0.001569	0.9913	0.0348
45	Y=0.0981X	0.0981	0.001434	0.9927	0.0654
60	Y=0.2243X	0.2243	0.005269	0.9905	0.1104
75	Y=0.2758X	0.2758	0.002674	0.9962	0.0915
90	Y=0.4377X	0.4377	0.010101	0.9907	0.1417

SS_{resid}: the residual sum of squares.

reaction mixture for 8 h without catalyst filtration produced a conversion level of 79.9%.

These results show that leaching of vanadium species from the catalyst sample during the liquid phase reaction was low and the catalyst was stable.

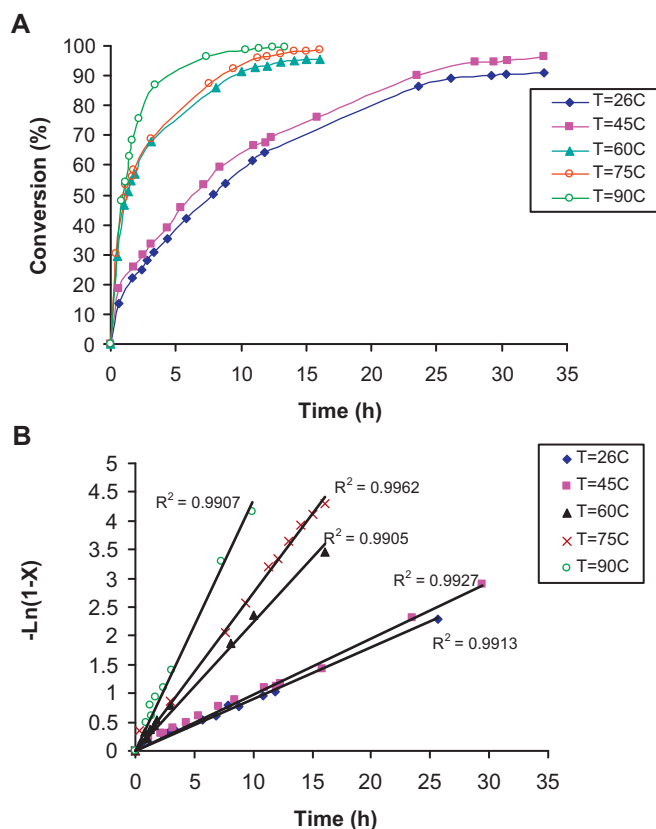


Fig. 7. (A) Conversion of benzyl alcohol as a function of time at 26, 45, 60, 75 and 90 °C with V₂O₅/K-OMS-2(2.30) catalyst in the presence of excess TBHP. (B) Pseudo-first order kinetics of benzyl alcohol oxidation at 26, 45, 60, 75 and 90 °C with V₂O₅/K-OMS-2(2.30) catalyst in the presence of excess TBHP. Reaction condition: 15 mL acetonitrile; 0.2 g V₂O₅/K-OMS-2(2.30) catalyst with the grain size of 200–230 mesh; the stirring rate of the reaction mixture 750 cycle/min benzyl alcohol 10 mmol; oxidant 150 mmol.

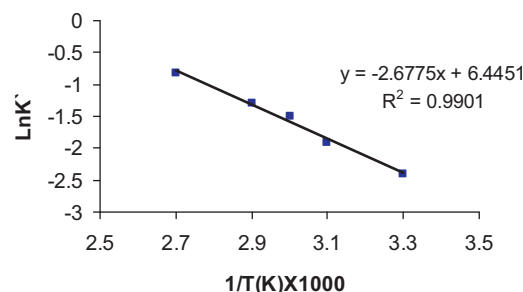


Fig. 8. Effect of temperature on the rate constant of the oxidation of benzyl alcohol (Arrhenius plot).

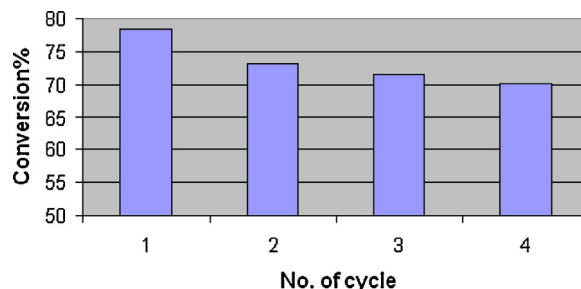


Fig. 9. The effect of catalyst recycling. Reaction condition: 0.2 g V₂O₅/K-OMS-2(2.30) catalyst; reflux temperature (90 °C); alcohol 30 mmol; oxidant 30 mmol; 15 mL acetonitrile; reaction time of a run 8 h.

Recycling potential was studied according to the following method; the catalyst was separated from the reaction mixture after each experiment by filtration, washed with solvent and dried carefully before using it in the subsequent run. The catalyst was used for four cycles and there was a progressive loss of activity with a lowering in conversion of benzyl alcohol (without any loss in selectivity) that indicated that leaching of vanadium species from the support had taken place. Therefore, the amount of vanadium loading was decreased in the sample and the activity of the catalyst in the next cycle decreased. The results are shown in Fig. 9. Conversion with only 8% reduction was observed after four cycles. Therefore, these results show that the potential reusability of the catalyst is appropriate.

4. Conclusion

In summary, the V₂O₅/K-OMS-2 samples with high V/Mn molar ratio were synthesized and used for the first time in reactions, for the oxidation of alcohols with *tert*-butyl hydroperoxide (TBHP) in the liquid phase. These new solids were composed of mixed phases of cryptomelane and crystalline V₂O₅. The results of catalytic tests showed that the vanadium impregnated catalyst had greatly enhanced catalytic activity respect to OMS-2 sample due to the interaction of manganese oxide and V₂O₅. The V₂O₅/K-OMS-2(2.30) was most active in catalyzing the oxidation of various alcohols with a good conversion percentage and selectivity by using TBHP as the oxidant.

In addition, the catalyst was recycled several times without any loss in selectivity and with a nearly identical conversion percentage of the recovered catalyst and this result suggests good reusability potential and stability. Another important consideration is that alkyl peroxides are very efficient oxidants and as the only by-products are alkyl alcohols they are not considered environmentally harmful. Therefore this system of catalysis is very suitable for the oxidation of alcohols. The kinetic of benzyl alcohol oxidation was investigated and results show that it followed a pseudo first order with respect to benzyl alcohol and the

mechanism of the reactions is under investigation in this laboratory.

References

- [1] R.A. Sheldon, J.K. Kochi, *Metal-Catalyzed Oxidations of Organic Compounds*, Academic Press, New York, 1994.
- [2] P.R.H.P. Rao, A.V. Ramaswamy, P. Ratnasamy, *J. Catal.* 141 (1993) 604–611.
- [3] K.R. Reddy, A.V. Ramaswamy, P. Ratnasamy, *J. Catal.* 143 (1993) 275–285.
- [4] P.R.H.P. Rao, A.V. Ramaswamy, P. Ratnasamy, *J. Chem. Soc. Chem. Commun.* (1992) 1245–1246.
- [5] A.V. Ramaswamy, S. Sivasanker, *Catal. Lett.* 22 (1993) 239–249.
- [6] J.S. Reddy, A. Sayari, *Catal. Lett.* 28 (1994) 263–267.
- [7] Y.F. Shen, P.R. Zerger, R.N. DeGuzman, S.L. Suib, L. McCurdy, D.I. Potter, C.L. O'Young, *Science* 260 (1993) 511–516.
- [8] Z.R. Tian, W. Tong, J.Y. Wang, N.G. Duan, V.V. Krishnan, S.L. Suib, *Science* 276 (1997) 926–930.
- [9] Z.R. Tian, Y.G. Yin, S.L. Suib, C.L. O'Young, *Chem. Mater.* 9 (1997) 1126–1133.
- [10] J.Y. Wang, G.G. Xia, Y.G. Yin, S.L. Suib, C.L. O'Young, *J. Catal.* 176 (1998) 275–284.
- [11] Y.C. Son, V.D. Makwana, A. Howell, S.L. Suib, *Angew. Chem. Int. Ed.* 40 (2001) 4280–4283.
- [12] S.L. Brock, N. Duan, Z.R. Tian, O. Giraldo, H. Zhou, S.L. Suib, *Chem. Mater.* 10 (1998) 2619–2628.
- [13] R.N. DeGuzman, Y.F. Shen, E.J. Neth, S.L. Suib, C.L. O'Young, S. Levine, J.M. Newsam, *Chem. Mater.* 6 (1994) 815–821.
- [14] Y.G. Yin, W.Q. Xu, R.N. DeGuzman, S.L. Suib, C.L. O'Young, *Inorg. Chem.* 33 (1994) 4384–4389.
- [15] N.G. Duan, S.L. Suib, C.L. O'Young, *J. Chem. Soc. Chem. Commun.* 13 (1995) 1367–1368.
- [16] V. Maraval, J.E. Ancel, B. Meunier, *J. Catal.* 206 (2002) 349–357.
- [17] A. Zsigmond, A. Horvath, F. Notheisz, *J. Mol. Catal. A* 171 (2001) 95–102.
- [18] S.P. Varkey, C. Ratnasamy, P. Ratnasamy, *J. Mol. Catal. A: Chem.* 135 (1998) 295–306.
- [19] V.D. Makwana, Y.C. Son, A.R. Howell, S.L. Suib, *J. Catal.* 210 (2002) 46–52.
- [20] X. Chen, Y.F. Shen, S.L. Suib, C.L. O'Young, *J. Catal.* 197 (2001) 292–302.
- [21] R.N. DeGuzman, Y.F. Shen, S.L. Suib, B.R. Shaw, C.L. O'Young, *Chem. Mater.* 5 (1993) 1395–1400.
- [22] J.B. Condon, *Surface Area and Porosity Determinations by Physisorption: Measurements and Theory*, Elsevier Science Ltd., Amsterdam, 2006.
- [23] R. Ghosh, Y.C. Son, V.D. Makwana, S.L. Suib, *J. Catal.* 224 (2004) 288–296.
- [24] V.D. Makwana, L. Garces, J. Liu, J. Cai, Y.C. Son, S.L. Suib, *Catal. Today* 85 (2003) 225–233.
- [25] V. Mahdavi, M. Mardani, M. Malekhosseini, *Catal. Commun.* 9 (2008) 2201–2204.
- [26] M.H. Peyrovi, V. Mahdavi, M.A. Salehi, R. Mahmoodian, *Catal. Commun.* 6 (2005) 476–479.
- [27] D. Brunel, F. Fajula, J.B. Nagy, B. Deroide, M.J. Verhoef, L. Veum, J.A. Peters, H.V. Bekkum, *Appl. Catal. A* 213 (2001) 73–82.
- [28] A.M. Khenkin, R. Neumann, *J. Org. Chem.* 67 (2002) 7075–7079.
- [29] B.Z. Zhan, M.A. White, T.K. Sham, J.A. Pincock, R.J. Doucet, K.V.R. Rao, K.N. Robertson, T.S. Cameron, *J. Am. Chem. Soc.* 125 (2003) 2195–2199.
- [30] V.R. Choudhary, P.A. Chaudhari, V.S. Narkhede, *Catal. Commun.* 4 (2003) 171–175.
- [31] T.L. Stuchinskaya, I.V. Kozhevnikov, *Catal. Commun.* 4 (2003) 417–422.
- [32] G. Ferguson, A. Nait Ajjou, *Tetrahedron Lett.* 44 (2003) 9139–9142.
- [33] R. Ganesan, B. Viswanathan, *J. Mol. Catal. A* 181 (2002) 99–107.
- [34] V.R. Choudhary, D.K. Dumbre, B.S. Uphade, V.S. Narkhede, *J. Mol. Catal. A* 215 (2004) 129–135.
- [35] A. Kockritz, M. Sebek, A. Dittmar, J. Radnik, A. Bruckner, U. Bentrup, H. Hugl, W. Magerlein, *J. Mol. Catal. A* 246 (2006) 85–99.
- [36] J.W. Moore, R.G. Pearson, *Kinetics and Mechanism*, John Wiley & Sons, Inc., New York, 1981.